PNAS NEXUS

PNAS Nexus, 2025, 4, pgaf025
https://doi.org/10.1093/pnasnexus/pgaf025
Advance access publication 27 January 2025
Research Report

Behavior changes influence mpox transmission in the United States, 2022–2023: Insights from homogeneous and heterogeneous models

Wei Zhang[a,b], Juan Zhang[c], Quan-Hui Liu[d], Shi Zhao[e], Wei-Qiang Li[b], Jun-Jie Ma[b], Xin Lu[f], Stefano Boccaletti[g,h,i] and Gui-Quan Sun[b,c,*]

[a]Data Science and Technology, North University of China, Taiyuan, Shanxi 030051, China
[b]School of Mathematics, North University of China, Taiyuan, Shanxi 030051, China
[c]Complex Systems Research Center, Shanxi University, Taiyuan, Shanxi 030006, China
[d]College of Computer Science, Sichuan University, Chengdu, Sichuan 610065, China
[e]School of Public Health, Tianjin Medical University, Tianjin 300070, China
[f]College of Systems Engineering, National University of Defense Technology, Changsha, Hunan 410073, China
[g]Sino-Europe Complex Science Center, North University of China, Taiyuan, Shanxi 030051, China
[h]CNR - Institute of Complex Systems, Via Madonna del Piano 10, Sesto Fiorentino I-50019, Italy
[i]Research Institute of Interdisciplinary Intelligent Science, Ningbo University of Technology, Ningbo, Zhejiang 315104, China
*To whom correspondence should be addressed: Email: gquansun@126.com
Edited By Attila Szolnoki

Abstract

In 2022, an unprecedented mpox epidemic rapidly swept the globe, primarily transmitted through sexual contact among men who have sex with men (MSM). However, our understanding of how changes in human behavior influence this outbreak remains incomplete. In this study, we introduce a two-layer network model to investigate the impact of human behavior on mpox transmission within the United States during 2022–2023, leveraging surveillance data. We theoretically explore mpox transmission under behavioral changes using homogeneous and heterogeneous mean-field approximations. While the heterogeneous model captures differences in individual behavior, its variations do not significantly affect the overall spread, validating the feasibility of using only homogeneous models to study behavioral changes. Utilizing infection data, we exhibit the influence of behavior changes across varying transmission levels of mpox, emphasize the significant role of sexual behavior among MSM, and recommend enhancing surveillance of nonsexual cases to enable timely control of spread. Utilizing vaccination data, we demonstrate the critical impact of behavior changes on the transmission capacity of mpox virus, contrasting the limited effectiveness of vaccine campaigns. This study highlights the importance of human behavior in controlling the spread of future outbreaks, offering valuable insights for the strategic development of public health interventions aimed at mitigating such occurrences.

Keywords: mpox, human behavior, sexual contact, multilayer network, vaccine campaigns

Significance Statement

We present a novel mathematical framework that explores the role of human behavior in the 2022–2023 mpox outbreak in the United States. Our findings underscore the validity of a homogeneous model in capturing behavior changes associated with this unusual outbreak, primarily transmitted through sexual contact. Our analysis reveals the significant impact of behavior changes on epidemic transmission dynamics, especially among men who have sex with men. It emphasizes that behavior changes, rather than vaccination, are pivotal in slowing the spread of the mpox virus in the United States.

Introduction

The emergence and spread of infectious diseases pose significant threats to public health worldwide. Understanding the underlying factors driving disease transmission is crucial for developing effective control strategies and mitigating the impact of outbreaks. In particular, human behavior plays a pivotal role in shaping the dynamics of disease spread, influencing contact patterns, transmission rates, and population susceptibility.

Since 2022 May 7, successive unprecedented outbreaks of human mpox ("mpox" following the name given on 2022 November

Competing Interest: The authors declare no competing interests.
Received: June 13, 2024. **Accepted:** January 2, 2025

28 by the World Health Organization [WHO] (1)) took place in Europe and the Americas, and spread across the globe (2–5). It was the first time that an outbreak of mpox appeared in nonendemic countries, with many cases and clusters in very different geographical regions (6). Although the first case was detected in the United Kingdom on 2022 July 25, the United States was declared to be the country with the most severe outbreak in the world.

Mpox is a zoonotic ailment caused by the mpox virus (MPXV). It spreads through various means, including direct contact with infected skin lesions or mucous membranes, droplet transmission, and contact with contaminated environments. While there is currently no evidence to classify mpox as a sexually transmitted disease, transmission through direct contact with compromised skin during sexual intercourse is a plausible route (7). Recent epidemiological investigations suggest that sexual contact primarily drove the transmission of mpox in 2022, contributing significantly to the widespread outbreak (8–14). Moreover, data indicate that the majority of cases in the ongoing mpox epidemic in the United States involve men who have sex with men (MSM) (15), thus underscoring the need to investigate the impact of human behavior on the atypical mpox epidemic.

Most literature studying mpox has focused on transmission between animals and humans (16–20) and co-infection models with other infectious disease (21). In addition, there is literature on other approaches to establish models about the transmission of mpox, such as stochastic model (22), deep learning models (23), heavy-tailed distribution (24), and optimal control (25), among others. There is, however, a paucity of models incorporating sexual behavior due to the distinct transmission dynamics observed in this outbreak compared with previous ones.

Epidemiological models for studying infectious diseases generally fall into two categories: homogeneous models assuming uniform mixing, and heterogeneous models considering varied contact network structures (26–29). For investigating mpox, compartmental models have been developed, categorizing populations into high- and low-risk groups, revealing that the high-risk group primarily drives mpox transmission in certain regions (30). Additionally, sexual transmission networks have been constructed for individuals who engage in sexual activity, demonstrating that MPXV infection risk in the United States for this group correlates significantly with the number of sexual partners (15). To further explore mpox development in the United States, we here propose accounting simultaneously for homogeneous and heterogeneous models, i.e. integrating diverse infection populations and transmission routes.

A growing body of evidence underscores the critical role of individual behavior during epidemic outbreaks, where people can spontaneously alter their actions to reduce the risk of disease transmission (31). Behavioral epidemiology specifically focuses on individual behaviors as determinants of the infection process. While the significance of human behavior is often embedded within patterns of social or sexual contact, these patterns are frequently treated as fixed constants, particularly in the context of vaccination, where behavior is assumed to be unaffected by the disease status (32). Reconstructing the social networks and individual health conditions during the 2009 H1N1 pandemic revealed that decisions to vaccinate were often influenced by whether friends had contracted influenza or had themselves decided to get vaccinated (33). Game theory has been employed to explore how individual imitation behaviors and group structures impact vaccination decisions within social networks, demonstrating how peer influence shapes these choices (34). By considering the cost and efficacy of vaccines, it was discovered that hysteresis loops can emerge in social imitation dynamics (35). Additionally, evolutionary game theory has been applied to study voluntary vaccination policies aimed at mitigating the severity of infectious diseases (36, 37). Given the importance of human behavior during the US mpox outbreak, we incorporate actual behavioral changes to explore its role in shaping the trajectory of the epidemic.

Given the escalating severity of the worldwide epidemic, particularly the rapid surge in cases within the United States, prompt government interventions are imperative to swiftly curtail the spread of the epidemic. With many nations implementing, at that time, travel restrictions and robust public health measures for COVID-19, the relatively low incidence of reported cases in the Western Pacific region underscores the efficacy of ongoing policy interventions in mitigating the spread of MPXV (38). However, while the disease appears to be manageable, the potential for it to spiral out of control persists in the absence of appropriate interventions (39). In response to the situation in the United States, on 2022 August 4, the government declared MPXV a "public health emergency." This declaration facilitated the release of emergency funding, granted federal agencies access to vital resources, streamlined the allocation of funds, and removed bureaucratic impediments hindering the containment of MPXV. Concurrently, efforts were intensified to enhance the availability and distribution of the JYNNEOS vaccine (40, 41). Due to the lack of complete vaccination data in the United Kingdom, models trying to assess the role of vaccines in outbreaks assumed that vaccination rates were proportionate to group sizes (42), although real-world scenarios often diverge from this assumption. In our study, we model vaccine distribution in the United States based on actual data provided by the Centers for Disease Control and Prevention (CDC) regarding two-dose vaccination rates.

We first encompass the development of both homogeneous and heterogeneous spreading models to examine the influence of human behaviors and MSM populations on the MPXV epidemic. Subsequently, we refine a time-varying homogeneous dynamical model using data on confirmed cases and vaccinations from the CDC to evaluate the impact of human behaviors and vaccine campaigns, integrating nonpharmacological and pharmacological interventions from 2022 May to 2023 September. We further analyze the MPXV transmission potential under various risk scenarios and quantify the effects of vaccine campaigns.

Results

We investigated the role of sexual and nonsexual transmission among the MSM and non-MSM populations in the context of changing human behaviors, utilizing both homogeneous and heterogeneous mean-field approximations (see Materials and methods). Furthermore, we calculated the transmission risks of MPXV during the US epidemic and assessed the relative importance of behavioral changes compared with vaccination campaigns by applying a time-varying homogeneous model to real-world surveillance data.

Epidemic spreading on a two-layer network

In delving into the 2022 outbreak of mpox, we established a mpox transmission model on a double-layer network characterizing the contacts pattern of population. Unlike prior mpox outbreaks, this global epidemic underscored the significance of close human-to-human contacts, particularly sexual contact among MSM (43). However, sexual transmission can also occur in the non-MSM with lower

transmission potential (24, 44, 45). Therefore, our model accounts for both MSM and non-MSM population. In addition, the mpox transmits through nonsexual type of contacts as well, such as nonsexually related skin-to-skin contact, respiratory droplets, and contaminants, just with a smaller transmission risk compared with the sexual contact (24, 46). To comprehensively explore the role of contact behavior in MPXV transmission, we then proposed a double-layer network consisting of layer A and layer B, which respectively represent the sexual contact network and the nonsexual contact network of the population (see Fig. 1). Note that one individual in the layer A corresponds to a unique node in layer B, and both the MSM population and non-MSM population exist in both layers. For simplicity, we assumed that there are no sexual contacts between individuals in the MSM population and individuals in the non-MSM population in layer A (24), while members of the two populations may have nonsexual contacts in layer B.

Each layer contains N nodes, where MSM individuals account for $N_1 = qN$ nodes, and non-MSM individuals for $N_2 = (1-q)N$ nodes, with q representing the proportion of MSM in the total population. It is well established that real-world sexual networks are highly heterogeneous, with the number of individual partners typically following a power-law distribution, $P_A(k) \sim k_A^{-\gamma}$, where k_A is the degree of a node in layer A (47–49). Based on empirical data and network structures, we set $\gamma_1 = 1.7$, $k_1^{\min} = 1$, $k_1^{\max} = 100$ for the MSM sexual network, $P_1(k) \sim k_1^{-\gamma_1}$, and $\gamma_2 = 3.5$, $k_2^{\min} = 1$, $k_2^{\max} = 20$ for the non-MSM sexual network, $P_2(k) \sim k_2^{-\gamma_2}$ (48, 49). For the nonsexual contact network, we assume a uniformly mixed population (50), modeling layer B as an Erdős–Rényi (ER) network with an average degree of $\langle k_3 \rangle = 20$, derived from empirical data (51).

To properly model the real-world spread of mpox in the United States, we propose a susceptible-exposed-infected-vaccinated-removed (SEIVR) epidemic model. In this network system, each node represents a distinct state (S, E, I, V_1, V_2, or R) of an individual. The transition between states arises from various events during epidemic spreading. Specifically, node S (or node V_1 or node V_2) transitions to node E following an infection event occurring upon contact with node I (i.e. $S \to E$, $V_1 \to E$, or $V_2 \to E$). Subsequently, an exposed node spontaneously progresses to an infected state through a transition event (i.e. $E \to I$), followed by removal from the infected pool via a removal event (i.e. $I \to R$). Additionally, node S undergoes a vaccination event to receive the first dose, transitioning to node V_1 (i.e. $S \to V_1$), followed by a second vaccination event to receive the second dose, transitioning to node V_2 (i.e. $V_1 \to V_2$). The epidemic process concludes when no infected nodes remain in the networks. More details on the spreading process in the two-layer network and a specific description of the model parameters can be found in the SI Appendix, Sections S1 and S2.

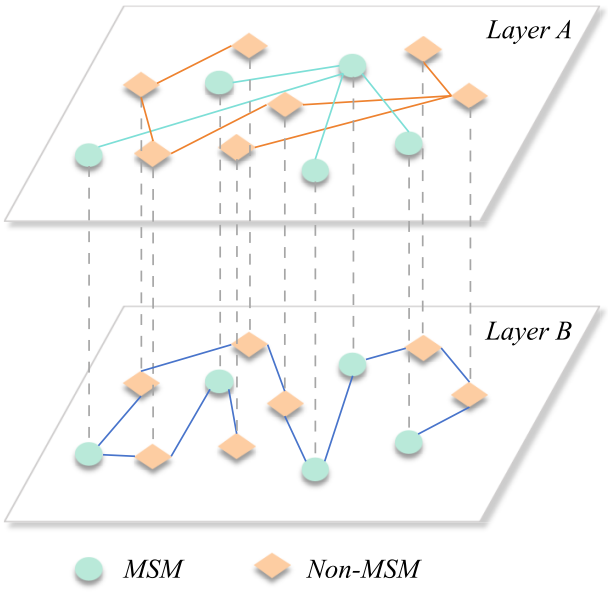

Fig. 1. Schematic illustration of the two-layer network. Each layer consists of the MSM and non-MSM populations, with each node in layer A corresponding one-to-one with a node in layer B. Layer A illustrates the sexual contact network, where MSM individuals interact with other MSM individuals and non-MSM individuals interact with other non-MSM individuals. Layer B depicts nonsexual contact, which can occur between any individuals.

Effects of human behavior on epidemic outbreak

We initially focus on assessing how behaviors influence the epidemic outbreak using homogeneous and heterogeneous mean-field approximations, see Materials and methods. Figure 2a illustrates the trends in infected MSM, infected non-MSM individuals, and the final size under varying sexual transmission probabilities for MSM individuals (λ_s^m). It is evident that both the peak values in each group and the final sizes increase with the transmission probability λ_s^m, regardless of the approximation used. However, comparisons between the two approximation theories reveal differences in the final and peak values. The final size predicted by the homogeneous approximation is consistently larger than that obtained from the heterogeneous approximation. The peak sizes for MSM and non-MSM individuals vary based on the two approximations, showing uncertainty as the infection probability changes. When $\lambda_s^m = 0.1$, the peak values using the heterogeneous mean-field approximation are higher for both infected MSM and non-MSM groups. Conversely, at $\lambda_s^m = 0.3$ and $\lambda_s^m = 0.5$, the homogeneous approximation yields higher peak values. It is also clear that under the heterogeneous mean-field approximation, the infected population reaches its peak earlier and has a shorter duration to reach a steady state. Additionally, similar trends are observed for varying sexual transmission probabilities (λ_s^o) among non-MSM individuals, and for different non-sexual transmission probabilities (λ_n), see Fig. 2b and c). At the same time, altering the proportion of MSM, yields the same result (see SI Appendix, Section S5.1). In conclusion, from a vertical perspective, an increase in the three transmission probabilities—regardless of the chosen approximation—leads to higher outbreak peaks and final sizes. From a horizontal perspective, the heterogeneous approximation facilitates a faster spread of the epidemic within the network due to the heterogeneity of node degrees, allowing highly connected nodes to transmit the disease more rapidly.

Furthermore, we investigate the effects of varying sexual transmission probabilities (setting $\lambda_s^m = \lambda_s^o$), nonsexual transmission probability (λ_n), and the proportion of MSM individuals (q) on the final infectious size, as shown in Fig. 3. The probability of nonsexual transmission is less influenced by q, and the final size increases steadily with rising nonsexual transmission. In contrast, the impact of sexual transmission probability on final size is complex and contingent upon the value of q. A more detailed analysis will be provided in the next section. Under both homogeneous and heterogeneous approximation theories, the trends in final size concerning transmission probabilities and proportions of MSM remain consistent. Additionally, we employ an event-driven algorithm to simulate the spreading process within a double-layer network, which further supports the observed trends in final size under different infection probabilities (see SI Appendix, Section S5.1).

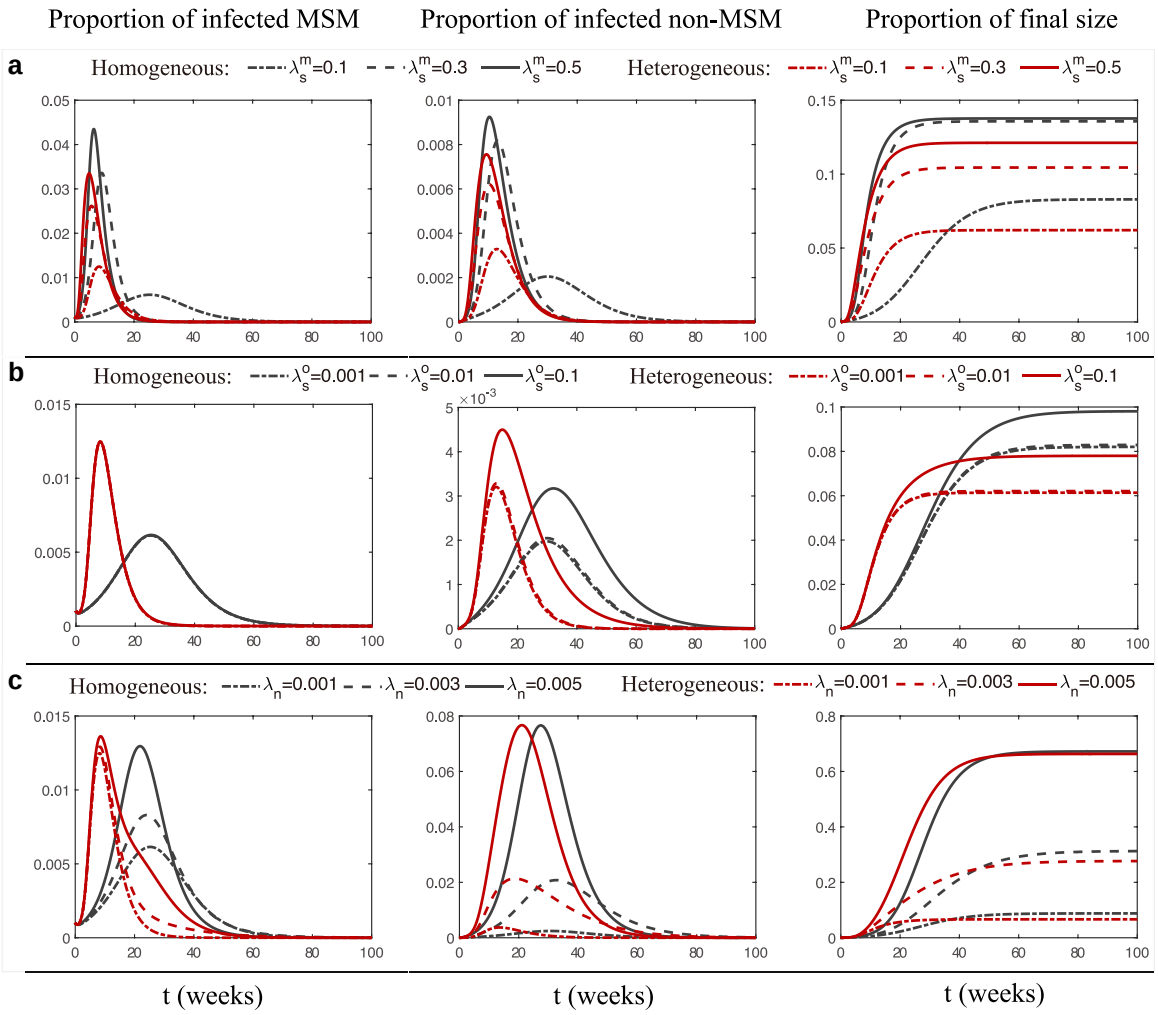

Fig. 2. The impact of human behaviors on the fraction of infectious outbreak size. Panel a) shows the effects of changes in the probability of sexual transmission within the MSM group (λ_s^m) on the proportion of infected MSM individuals, infected non-MSM individuals, and total outbreak size, respectively. Panel b) illustrates the effects of changes in the sexual transmission probability (λ_s^o) within the non-MSM group. Panel c) displays the effects of changes in the nonsexual transmission probability (λ_n). The different curves represent the results from the homogeneous mean-field model (Eq. 1) and the heterogeneous mean-field model (Eq. 4), respectively. Other transmission probabilities are set as $\lambda_s^o = 0.01$ and $\lambda_n = 0.001$ in (a), $\lambda_s^m = 0.1$ and $\lambda_n = 0.001$ in (b), and $\lambda_s^m = 0.1$, $\lambda_s^o = 0.05$ in (c). Additional model parameters are $q = 0.1$, $w = 1$, $\delta = 1/3$, $\epsilon_1 = 1 - 0.752$, $\epsilon_2 = 1 - 0.859$, $\phi_1 = \phi_2 = 0.002$, and $\psi_1 = \psi_2 = 0.6$ (see SI Appendix, Section S2).

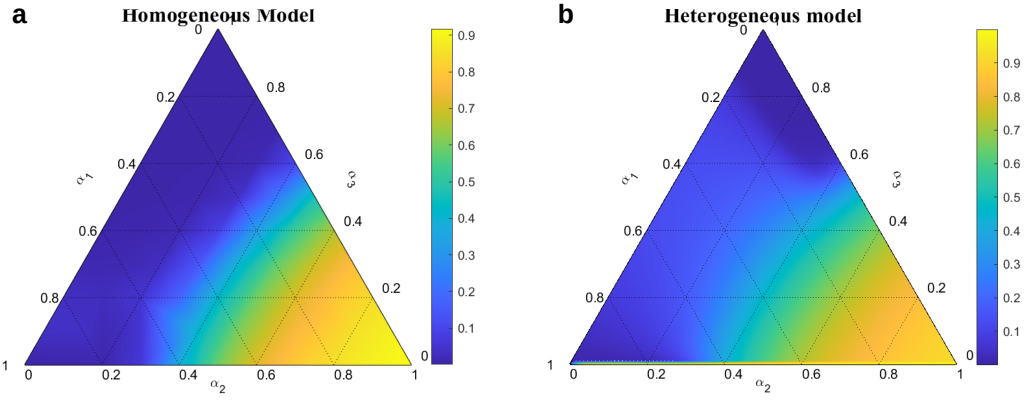

Fig. 3. The influence of sexual and nonsexual behaviors, and MSM population on the infectious outbreak size. Panels a) and b) illustrate the effects of varying the sexual transmission probability (λ_s^m), nonsexual transmission probability (λ_n), and the proportion of MSM individuals (q) on the fraction of the infectious outbreak. Panel a) shows the simulation results based on the homogeneous mean-field approximation, while panel b) presents results from the heterogeneous mean-field approximation. For varying parameters α_1, α_2, and α_3, we set $\lambda_s^m = \alpha_1/10$, $\lambda_n = \alpha_2/100$, and $q = \alpha_3$. The additional parameters used are $\lambda_s^o = \lambda_s^m$, $w = 1$, $\delta = 1/3$, $\epsilon_1 = 1 - 0.752$, $\epsilon_2 = 1 - 0.859$, $\phi_1 = \phi_2 = 0.002$, and $\psi_1 = \psi_2 = 0.6$.

Behavioral shifts influence how frequently, for how long, or how individuals are in contact with each other, thereby altering the likelihood of epidemic spread. Specifically, when individuals reduce social interactions (e.g. limiting social activities), the transmission probability drops, decreasing the risk of disease transmission. Similarly, adopting protective measures, such as wearing condoms, using sterilization, or maintaining social distance, lowers the transmission probability per exposure, even if contact still exists. Thus, for both the homogeneous and heterogeneous models, while the numerical values of outbreak peak and final sizes differ slightly, the overall trends in response to changes in human behavior remain consistent (see Materials and Methods). Since our two-layer network system is static, human behavior is typically reflected through changes in transmission probability. Our study highlights that, despite the heterogeneous nature of individual behavior, the role of individual behavior is similar to that of collective behavior, which does not significantly influence the effects of behavioral changes on the spread of the mpox epidemic.

Effects of human behavior on MPXV transmission potential

We examine the influence of human behavior and MSM populations on the transmission potential of MPXV using the basic reproduction number (R_0) as the metric (see SI Appendix, Section S4). To analyze how different factors affect transmission potential, we separately explore the impact of specific types of contact and the proportion of MSM individuals. Figure 4a shows the results under the homogeneous mean-field model. One finds that there is a proportional relationship between the transmission

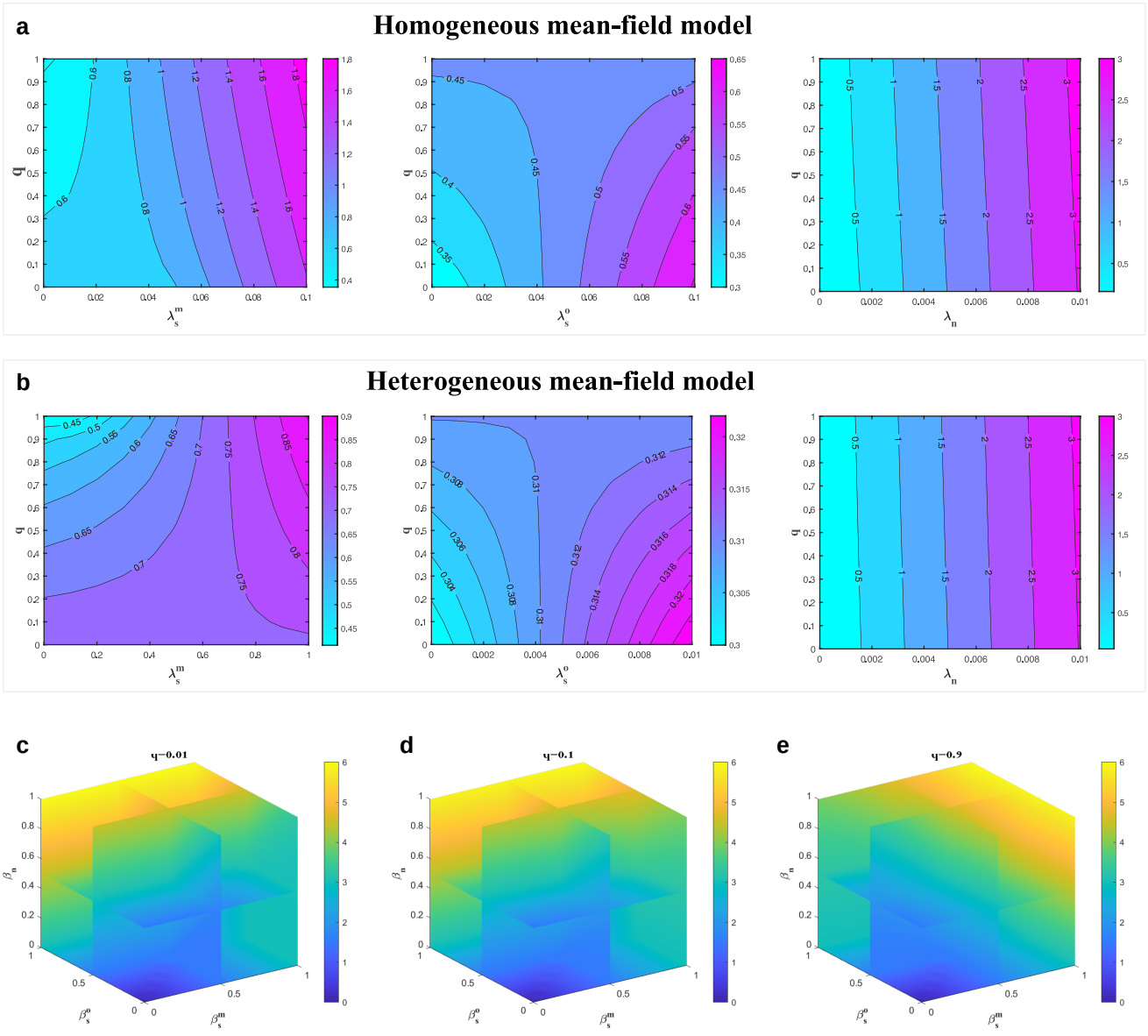

Fig. 4. The impact of human behaviors and the MSM population on the basic reproduction number. Panel a) displays the results from the homogeneous mean-field approximation, while panel b) present results from the heterogeneous mean-field approximation. In the first column of (a) and (b), it is about the effect of λ_s^m and q on basic reproduction number R_0, the other transmission probabilities are $\lambda_s^o = 0.1$ and $\lambda_n = 0.001$; in second column, it is about the effect of λ_s^o and q, others are $\lambda_s^m = 0.01$ and $\lambda_n = 0.001$; in third column in (a), $\lambda_s^o = 0.01$ and $\lambda_s^m = 0.01$; and in third column of (b), $\lambda_s^o = 0.01$ and $\lambda_s^m = 0.1$. Panels c)–e) are three-dimensional stereograms. In the homogeneous model, we set $\beta_s^m = \lambda_s^m\langle k_1\rangle$, $\beta_s^o = \lambda_s^o\langle k_2\rangle$, and $\beta_n = \lambda_n\langle k_3\rangle$. The MSM population proportion (q) is set to 0.01, 0.1, and 0.9 in panels (c), (d), and (e), respectively. Other parameters are $\lambda_s^m = \lambda_s^o$, $w = 1$, $\delta = 1/3$, $\epsilon_1 = 1 - 0.752$, $\epsilon_2 = 1 - 0.859$, $\phi_1 = \phi_2 = 0.002$, and $\psi_1 = \psi_2 = 0.6$.

probabilities of sexual or nonsexual contact and R_0. However, the effect of the MSM population (q) on R_0 is not uniform across scenarios. We identify critical values where this relationship shifts in the first and second columns of Fig. 4a. Notably, in the first column of Fig. 4a, R_0 decreases as q increases when λ_s^m is below its critical value, but R_0 increases as q increases when λ_s^m rises above it. In contrast, the second column of Fig. 4a shows an opposite trend for λ_s^o: R_0 increases to the left of its critical value and decreases to the right. The influence of the MSM population q, therefore, depends on these critical points. The heterogeneous mean-field theory shows similar results, as shown in Fig. 4b, though with different critical values and R_0 magnitudes. In general, the homogeneous approximation yields higher R_0 values for the same parameter settings. All in all, as sexual and nonsexual transmission intensifies, the severity of MPXV spread worsens, and the role of the MSM population becomes more complex, with its impact shifting based on changes in sexual or nonsexual behavior.

Moreover, since behavioral changes exhibit consistent trends in both the homogeneous and heterogeneous models, we opt to use the homogeneous model to explore the combined effects of the three transmission rates (we denote $\beta_s^m = \lambda_s^m\langle k_1\rangle$, $\beta_s^o = \lambda_s^o\langle k_2\rangle$, and $\beta_n = \lambda_n\langle k_3\rangle$) and the proportion of MSM individuals (q) (see Fig. 4c–e). The simulation results reveal that the nonsexual transmission rate (β_n) significantly affects the basic reproduction number (R_0). The influence of β_s^m or β_s^o primarily depends on the size of q; as q increases, the impact of β_s^m becomes more pronounced. This underscores the need for enhanced surveillane od nonsexual cases to control transmission timely. Clearly, when the proportion of MSM individuals is high, reducing sexual behavior among MSM can effectively mitigate the transmission potential.

MPXV transmission risk in the United States in response to behavior changes

Our results indicate that the homogeneous model can effectively replicate the transmission characteristics observed in the heterogeneous model under varying behavioral conditions, thereby providing a rational validation for its use. Consequently, we utilized a time-varying homogeneous model (see Materials and methods) grounded in real surveillance data to analyze the actual spread of mpox in the United States from 2022 May to 2023 September.

We estimate the parameters in the time-varying homogeneous model using a least-squares approach (see the SI Appendix, Section S3). As mpox outbreaks evolve, behavioral changes impact transmission dynamics. We derive the transmission thresholds for MPXV under varying behavior and classify the transmission risk according to the size of this threshold. The basic reproduction number (R_0) for the period from 2022 May 28 to 2022 July 30 is estimated at 3.1186, indicating a high-risk transmission phase for mpox in the United States. From 2022 August 6 to 2023 May 6, the estimated R_0 is 0.4492, corresponding to a low-risk transmission phase. Finally, from 2023 May 13 to 2023 September 16, the R_0 is estimated at 1.7119, reflecting a medium-risk transmission phase. Figure 5a illustrates changes in transmission potential under different risk levels, such as high-, low- and medium-risk transmissions. These changes are based on the effective reproduction number (refer to the SI Appendix, Section S4.1). It reveals that the epidemic initially begin with a high-risk transmission, then shifted to a low risk due to human behavioral responses to governmental nonpharmacological and pharmacological interventions. Ultimately, the epidemic reaches an medium-risk phase as behaviors continued to evolve following the WHO's declaration on 2023 May 11 that MPXV was no longer considered a global health emergency.

In parallel, we analyze the sensitivity of the reproduction number (R_0) at each stage (see SI Appendix, Section S4.3), providing a theoretical basis and effective prevention for mitigating and controlling the spread of MPXV under different transmission risks. Pharmacological therapy, i.e. increasing the recovery rate δ, consistently emerges as important and effective in mitigating the transmission ability of MPXV. Furthermore, the most sensitive parameter for positively altering transmission potential under each-risk transmission is the sexual transmission rate in MSM group (β_s^m), whereas the rate of nonsexual transmission (β_n) becomes sensitive in the case of medium-risk transmission.

Behavior change outperforms the US vaccine campaign

To explore the crucial measures to curb the spread of the mpox epidemic in the United States, we compare the impact of human behavioral changes and vaccine campaigns. In actual spread scenarios, changes in human behavior directly influence the transmission rates (β_s^m, β_s^o, and β_n). Additionally, the proportion of MSM group (q) reflects the MSM infections following population infection as a result of human behavioral changes. Figure 5a shows that changes in the effective reproduction number first decrease and then increase due to complex shifts in human behavior. We have previously discussed the intricate interaction between behavior and proportion.

As the vaccination campaign progresses through different transmission stages, we find that the effective reproduction number decreases slightly (see SI Appendix, Section S5.2). We also investigate the impact of vaccine campaigns on the infectious population. Figure 5b–d illustrates the evolution of the number of MSM cases, non-MSM cases, and cumulative infected cases under different vaccine campaign scenarios. The $\phi = \phi(t)$ and $\psi = \psi(t)$ demonstrate a real United States vaccine campaign with specific values provided in the SI Appendix, Section S3.2. In addition, we simulate a scenario where only the MSM population was vaccinated (see SI Appendix, Section S5.3). Overall, vaccine campaigns have modest impact on MPXV transmission potential and infectious cases. Our findings emphasize that changes in human behavior have a significant effect on MPXV transmission potential, while vaccine campaigns only modestly reduce transmission risk during the 2022–2023 mpox epidemics in the United States. However, this does not diminish the importance of vaccines in controlling epidemic progression. As shown in Fig. 5b–d, a substantial increase in vaccination rates would effectively control infections. According to data from the CDC, vaccination has historically been a cornerstone of mpox prevention, with campaigns proving effective and long-lasting in curbing epidemics (52). Therefore, achieving higher vaccination coverage is essential for long-term mitigation and containment of mpox.

Discussion

The atypical outbreak of mpox in the United States in 2022 marked a departure from previous occurrences, shifting from pet-related outbreaks to human-to-human transmission, particularly among individuals engaged in sexual behavior. In the early stages of the mpox outbreak, public awareness of self-protection was limited, contributing to exponential growth in infections despite government vaccination efforts. It was not until August 4 that the Secretary of Health and Human Services declared the outbreak a public health emergency, after which the rate of growth began to slow, likely influenced by factors such as vaccination, behavioral changes, and increased immunity within the MSM

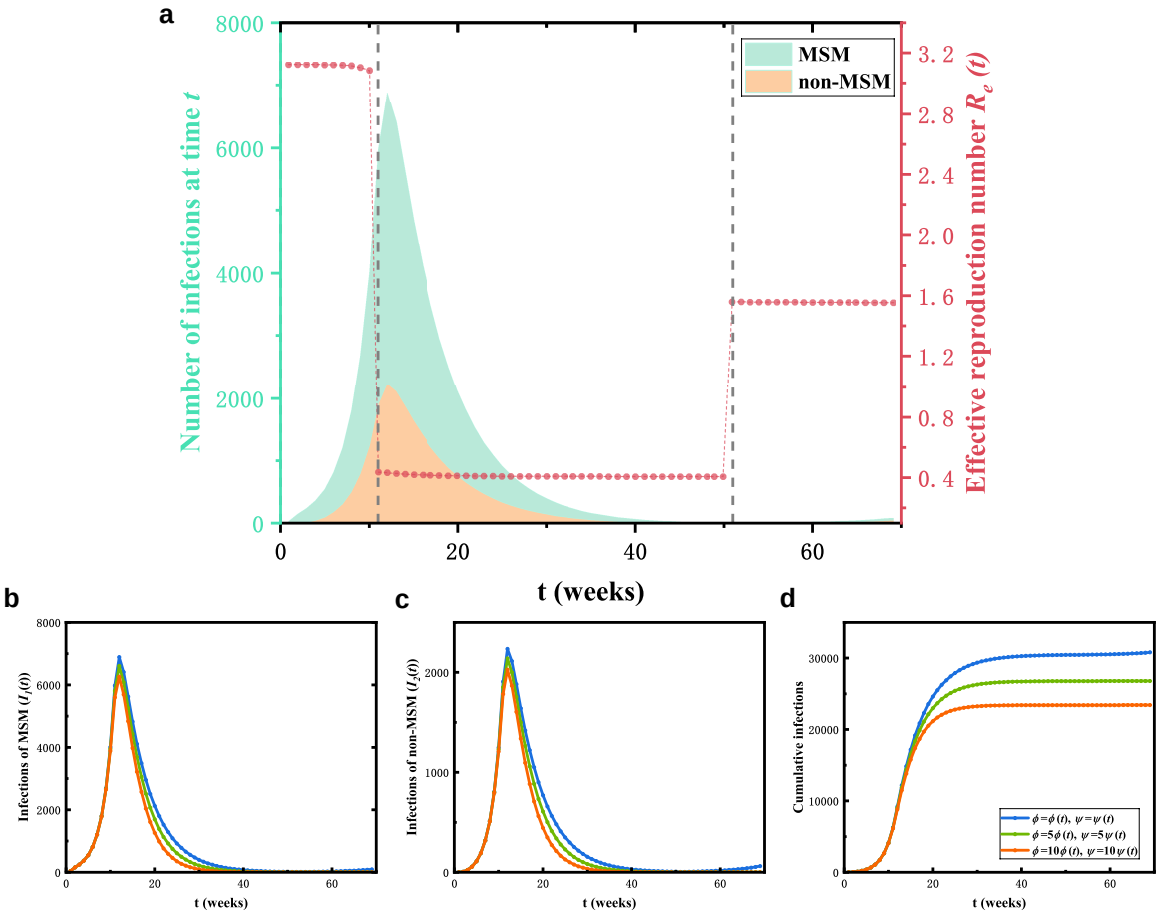

Fig. 5. The transmission potential and infectious population of mpox in the United States from the first week starting 2022 May 28, to the 69th week ending 2023 September 16. In panel a), the left side depicts the evolution of the infectious cases among the MSM and non-MSM population. The dashed line represents the segment nodes of the time-varying model (refer to Materials and methods). The right side displays the MPXV transmission risk, with the dot marking the effective reproduction number. Panels b)–d) depict the number of infections among the MSM and non-MSM populations, as well as cumulative infections, under different vaccination conditions. Where ϕ and ψ are the numbers of first and second doses of vaccination, respectively. Model parameter values for different transmission risks are detailed in the SI Appendix, Section S3.

population. However, both the CDC and the UK Health Security Agency suggest that vaccination alone is unlikely to account for the decline in reproduction numbers below one (53).

Our research examines mpox transmission by analyzing how different human behaviors interact within a two-layer network model, applying both homogeneous and heterogeneous approximations. While the peak values and epidemic sizes differ slightly between the models, the overall trends in response to behavioral changes remain consistent. Our results reveal that changes in individual behavior, in contrast to changes in collective behavior, do not significantly affect the trends in mpox transmission. This validates the feasibility of homogeneous models for studying mpox transmission under behavioral changes. This supports the feasibility of employing homogeneous methods to study mpox transmission in the context of behavioral changes. Additionally, both sexual and nonsexual behaviors are closely linked to the size of the MSM population regarding virus transmission control. Apparently, reducing sexual activity among a high proportion of MSM can effectively lower transmission potential. Furthermore, nonsexual behaviors across all populations significantly influence MPXV transmission capacity, highlighting the need to enhance surveillance of nonsexual cases to control transmission effectively.

In addition, we found that the lack of successive implementation of interventions led to a return to the intensity of sexual behavior. Accordingly, a suggestion may be given to focus on protecting GBMSM groups under high- and medium-risk transmissions, which could effectively mitigate the ability of MPXV to spread and substantially reduce its infections. The major government measures to reduce sexual include media campaigns to raise awareness of self-protection and the adoption of vaccination strategies. As the epidemic progresses, even those who are not sexually active may be at risk of infection (50). We therefore recommend that intervention policies prevent nonsexual behavior along with reducing sexual behavior under medium-risk transmissions. Otherwise, epidemic will rebound, as it happened when the WHO declared the lifting of the state of emergency for mpox on 2023 May 11.

Furthermore, our findings demonstrated that human behavior changes had a significantly stronger impact than vaccine campaigns in controlling the spread of mpox outbreaks in 2022–2023. Vaccine campaigns in the United States effectively but modestly altered transmission potential, aligning with CDC reports that the vaccine played a limited role in significantly reducing R_0 (53). Compared to direct vaccination with the first dose and no vaccination, however, the impact on the spread and eventual size of the outbreak was small. The phenomenon occurs because of insufficient vaccine coverage, and when the number of vaccinations is significantly increased, a remarkable reduction in the size of the infection is observed. Vaccination campaigns have been shown to be an effective and long-term validity tool in mitigating

mpox epidemics (52). Consequently, we find it necessary to recommend rapid and sustained interventions.

In our study, we assumed constant transmission rates and proportions of infected GBMSM groups within the same transmission risks, overlooking their potential variability. While incorporating time-varying parameter values offers greater realism, the lack of real-time monitoring of transmission rates means that we still assume the constancy of parameter values at each stage of risk transmission. Additionally, because our focus was on examining the influence of human behavior on mpox outbreaks and transmission, we did not account for presymptomatic infected individuals or external imported cases in modeling approach. For countries and regions at risk of importation, we simulate the impact of different scales of imported cases on the final size of the outbreak, which will eventually lead to only small outbreaks under different country and regional responses to the Strategic Preparedness, Readiness, and Response Plan (SPRP) of the WHO, see SI Appendix, Section S5.4. Obviously, this brings a great challenge to low-income countries and settings as well (54). The advantages of rapid and sustained government intervention against the MPXV, reducing the chances of evolution and benefiting both local communities and the world (39). Meanwhile, self-protection awareness, public education, and vaccine campaigns can help government departments prevent localized outbreaks on the one hand and minimize the risk to individuals on the other, which is crucial for countries where new cases are expected to emerge (38).

In the early stages of our work, we thoroughly examined how different behavioral changes impact mpox transmission using homogeneous and heterogeneous approximation theories. Later, we gained real-world insights by fitting time-varying homogeneous models to actual data, balancing theoretical exploration with practical application. By discussing heterogeneity, we avoid premature simplifications and ensure a comprehensive and rigorous understanding of how behavioral changes influence MPXV transmission. Homogeneous models provide insight into overall spread trends when most individuals adopt similar measures, while heterogeneous models highlight the effects of key individuals when their behaviors change. In future research, we aim to explore more complex network structures, such as dynamic networks, and investigate more intricate heterogeneous behaviors, particularly in super-spreader scenarios, to better understand the role of behavioral changes.

In summary, we develop both the homogeneous modeling framework and the heterogeneous modeling framework to explore the impact of human behavior on mpox transmission. Our findings highlight the applicability of homogeneous modeling for qualitatively examining the influence of human behavior on atypical mpox outbreaks. Through the development of a time-varying homogeneous model utilizing reported case data and vaccination data from the United States, we examine the role of human behavior across various transmission risks scenarios and reveal that behavior change is superior to US vaccine campaigns in curbing the spread of mpox epidemic. Our study presents a homogeneous modeling framework with broad applicability for informing public health interventions aimed at mitigating future outbreaks.

Materials and methods

We analyze the impact of human behavioral changes on MPXV transmission by focusing on two critical metrics: the final infection size and the basic reproduction number. To predict these quantities in a two-layer network, we develop two theoretical frameworks—one based on a homogeneous mean-field approximation and the other on a heterogeneous mean-field perspective.

Homogeneous mean-field approximation

We define the variables $S_i(t)$, $E_i(t)$, $I_i(t)$, $R_i(t)$, $V_i^1(t)$, and $V_i^2(t)$ as the number of individuals who are susceptible, exposed, infected, removed, vaccinated with the first dose, and vaccinated with the second dose at time t, respectively. The index $i=1$ refers to MSM individuals, while $i=2$ represents non-MSM individuals. The total number of individuals in each group at time t is given by $N_i(t)=S_i(t)+E_i(t)+I_i(t)+R_i(t)+V_i^1(t)+V_i^2(t)$, and the total population at time t is $N(t)=N_1(t)+N_2(t)$.

To model the dynamics, we develop a homogeneous mean-field equation that describes the time evolution of these variables (see Eq. 1). We assume that $\lambda_s^m(t)$ denotes the infection probability within the MSM sexual contact network, $\lambda_s^o(t)$ denotes the infection probability of sexual contact network in non-MSM group, and $\lambda_n(t)$ denotes the infection probability of nonsexual contact network in all populations. The parameters $\langle k_1\rangle$, $\langle k_2\rangle$, and $\langle k_3\rangle$ denote the average degrees of the MSM sexual, non-MSM sexual, and nonsexual networks, respectively. Vaccination rates for receiving the first and second doses are denoted by ϕ_i and ψ_i, respectively, though the vaccines are not fully effective. Vaccinated individuals experience failure rates of ϵ_1 in $V_1(t)$ and ϵ_2 in $V_2(t)$. Exposed individuals progress to the infected state at a rate w, and infected individuals are removed at a rate δ.

$$
\begin{aligned}
\frac{dS_1(t)}{dt} &= -\phi_1 S_1(t) - \lambda_s^m\langle k_1\rangle S_1(t)\Theta_1'(t) - \lambda_n\langle k_3\rangle S_1(t)\Theta_3'(t),\\
\frac{dS_2(t)}{dt} &= -\phi_2 S_2(t) - \lambda_s^o\langle k_2\rangle S_2(t)\Theta_2'(t) - \lambda_n\langle k_3\rangle S_2(t)\Theta_3'(t),\\
\frac{dV_1^1(t)}{dt} &= \phi_1 S_1(t) - \psi_1 V_1^1(t) - \epsilon_1\lambda_s^m\langle k_1\rangle V_1^1(t)\Theta_1'(t) - \epsilon_1\lambda_n\langle k_3\rangle V_1^1(t)\Theta_3'(t),\\
\frac{dV_2^1(t)}{dt} &= \phi_2 S_2(t) - \psi_2 V_2^1(t) - \epsilon_1\lambda_s^o\langle k_2\rangle V_2^1(t)\Theta_2'(t) - \epsilon_1\lambda_n\langle k_3\rangle V_2^1(t)\Theta_3'(t),\\
\frac{dV_1^2(t)}{dt} &= \psi_1 S_1(t) - \epsilon_2\lambda_s^m\langle k_1\rangle V_1^2(t)\Theta_1'(t) - \epsilon_2\lambda_n\langle k_3\rangle V_1^2(t)\Theta_3'(t),\\
\frac{dV_2^2(t)}{dt} &= \psi_2 V_2^1(t) - \epsilon_2\lambda_s^o\langle k_2\rangle V_2^2(t)\Theta_2'(t) - \epsilon_2\lambda_n\langle k_3\rangle V_2^2(t)\Theta_3'(t),\\
\frac{dE_1(t)}{dt} &= (S_1(t)+\epsilon_1 V_1^1(t)+\epsilon_2 V_1^2(t))(\lambda_s^m\langle k_1\rangle\Theta_1'(t)+\lambda_n\langle k_3\rangle\Theta_3'(t)) - wE_1(t),\\
\frac{dE_2(t)}{dt} &= (S_2(t)+\epsilon_1 V_2^1(t)+\epsilon_2 V_2^2(t))(\lambda_s^o\langle k_2\rangle\Theta_2'(t)+\lambda_n\langle k_3\rangle\Theta_3'(t)) - wE_2(t),\\
\frac{dI_1(t)}{dt} &= wE_1(t) - \delta I_1(t),\\
\frac{dI_2(t)}{dt} &= wE_2(t) - \delta I_2(t),\\
\frac{dR_1(t)}{dt} &= \delta I_1(t),\\
\frac{dR_2(t)}{dt} &= \delta I_2(t),
\end{aligned}
\tag{1}
$$

where

$$
\begin{aligned}
\Theta_1'(t) &= \frac{I_1(t)}{N_1(t)},\\
\Theta_2'(t) &= \frac{I_2(t)}{N_2(t)},\\
\Theta_3'(t) &= \frac{I_1(t)+I_2(t)}{N(t)}.
\end{aligned}
\tag{2}
$$

Heterogeneous mean-field approximation

Let the variables $S_i^k(t)$, $E_i^k(t)$, $I_i^k(t)$ $R_i^k(t)$, $V_i^{1k}(t)$, and $V_i^{2k}(t)$ be, respectively, as the number of nodes being in susceptible, exposed, infected, removed, vaccinated with the first dose and vaccinated with the second dose of degree k in layer A at time t. The $i=1$ represents the number of MSM individuals, and $i=2$ denotes the number of non-MSM individuals. In particular, the total infections

at time t is $I_3(t) = I_1(t) + I_2(t)$, where $I_1(t) = \sum_k I_1^k(t)$ and $I_2(t) = \sum_k I_2^k(t)$. And the total population at time t is $N_3(t) = N_1(t) + N_2(t)$, where $N_1(t) = \sum_k N_1^k(t)$ is total number of MSM population and $N_2(t) = \sum_k N_2^k(t)$ is total number of non-MSM population. The $P_1(k)$ and $P_2(k)$ are the degree distributions of MSM sexual, non-MSM sexual networks in layer A with average degrees $\langle k_1\rangle$, $\langle k_2\rangle$, respectively. The $P(k)$ is a degree distribution of nonsexual network in layer B with average degrees $\langle k_3\rangle$. To model the epidemic, we develop the heterogeneous mean-field theory, taking into account uncorrelated double-layer networks. Thus, the probability that a susceptible individual has an infected neighbor in each network at time t is given by:

$$\begin{aligned}
\Theta_1(t) &= \sum_{k_1'} \frac{k_1' P_1(k_1')}{\langle k_1\rangle} \frac{I_1^{k_1'}(t)}{N_1^{k_1'}(t)},\\
\Theta_2(t) &= \sum_{k_2'} \frac{k_2' P_2(k_2')}{\langle k_2\rangle} \frac{I_2^{k_2'}(t)}{N_2^{k_2'}(t)},\\
\Theta_3(t) &= \sum_{k_3'} \frac{k_3' P(k_3')}{\langle k_3\rangle} \frac{I_3^{k_3'}(t)}{N_3^{k_3'}(t)}.
\end{aligned} \tag{3}$$

According to the construction of the double-layer system (see Fig. 1), a susceptible individual in the MSM group can be infected through both the sexual network of MSM and the nonsexual network involving the entire population. Similarly, a susceptible individual in the non-MSM group can be infected through the sexual network of non-MSM individuals and the nonsexual network shared by the entire population. Since the nonsexual network is modeled as an ER network, we simplify the model by assuming that the probability of a susceptible node of degree k being infected through nonsexual contact is independent of the degree k. Instead, it will only depends on the average degree, given by $\sum_{k_3} k_3 P(k_3)$. The other parameters remain consistent with those in the homogeneous model. Thus, the heterogeneous model is given by:

$$\begin{aligned}
\frac{dS_1^k(t)}{dt} &= -\phi_1 S_1^k(t) - \lambda_s^m k S_1^k(t)\Theta_1(t) - \lambda_n \sum_{k_3} k_3 P(k_3) S_1^k(t)\Theta_3(t),\\
\frac{dS_2^k(t)}{dt} &= -\phi_2 S_2^k(t) - \lambda_s^o k S_2^k(t)\Theta_2(t) - \lambda_n \sum_{k_3} k_3 P(k_3) S_2^k(t)\Theta_3(t),\\
\frac{dV_1^{1k}(t)}{dt} &= \phi_1 S_1^k(t) - \psi_1 V_1^{1k}(t) - \epsilon_1\lambda_s^m k V_1^{1k}(t)\Theta_1(t) - \epsilon_1\lambda_n \sum_{k_3} k_3 P(k_3) V_1^{1k}(t)\Theta_3(t),\\
\frac{dV_2^{1k}(t)}{dt} &= \phi_2 S_2^k(t) - \psi_2 V_2^{1k}(t) - \epsilon_1\lambda_s^o k V_2^{1k}(t)\Theta_2(t) - \epsilon_1\lambda_n \sum_{k_3} k_3 P(k_3) V_2^{1k}(t)\Theta_3(t),\\
\frac{dV_1^{2k}(t)}{dt} &= \psi_1 V_1^{1k}(t) - \epsilon_2\lambda_s^m k V_1^{2k}(t)\Theta_1(t) - \epsilon_2\lambda_n \sum_{k_3} k_3 P(k_3) V_1^{2k}(t)\Theta_3(t),\\
\frac{dV_2^{2k}(t)}{dt} &= \psi_2 V_2^{1k}(t) - \epsilon_2\lambda_s^o k V_2^{2k}(t)\Theta_2(t) - \epsilon_2\lambda_n \sum_{k_3} k_3 P(k_3) V_2^{2k}(t)\Theta_3(t),\\
\frac{dE_1^k(t)}{dt} &= (S_1^k(t) + \epsilon_1 V_1^{1k}(t) + \epsilon_2 V_1^{2k}(t))(\lambda_s^m k\Theta_1(t) + \lambda_n \sum_{k_3} k_3 P(k_3)\Theta_3(t)) - \omega E_1^k(t),\\
\frac{dE_2^k(t)}{dt} &= (S_2^k(t) + \epsilon_1 V_2^{1k}(t) + \epsilon_2 V_2^{2k}(t))(\lambda_s^o k\Theta_2(t) + \lambda_n \sum_{k_3} k_3 P(k_3)\Theta_3(t)) - \omega E_2^k(t),\\
\frac{dI_1^k(t)}{dt} &= \omega E_1^k(t) - \delta I_1^k(t),\\
\frac{dI_2^k(t)}{dt} &= \omega E_2^k(t) - \delta I_2^k(t),\\
\frac{dR_1^k(t)}{dt} &= \delta I_1^k(t),\\
\frac{dR_2^k(t)}{dt} &= \delta I_2^k(t).
\end{aligned} \tag{4}$$

Time-varying homogeneous model in response to behavior changes

Behavioral changes inducing variations in transmission rates

As an epidemic progresses, people's attitudes and responses to risk often shift, leading to spontaneous changes in behavior (31). These behavioral changes, in turn, can have a profound impact on the course of the epidemic (55). When the perception of risk is high, individuals are more likely to alter their contact patterns, which can help suppress the spread of the epidemic. Conversely, as perceived risk decreases, individuals often return to their previous behaviors (31). If the virus has not been eradicated and vaccine protection is insufficient, this could lead to a resurgence of the epidemic. It is clear that MPXV transmission is closely tied to changes in individual behavior. Accordingly, we assumed that these behavioral changes would result in alterations to the transmission rate for each infected individual (42).

Time-varying homogeneous model

Given our focus on the US situation from 2022 May to 2023 September, we adapt the homogeneous model structure based on confirmed data and actual US government responses. The first confirmed case of mpox in the United States was reported in Massachusetts on May 18, with the first death confirmed in California on September 12. While cases of mpox were initially detected in Europe in 2022, the United States had reported 3,846 confirmed cases as of July 25, making it the country with the highest number of mpox cases worldwide, according to data released by the CDC. However, it was not until August 4th that the US government declared mpox a "public health emergency," aimed at raising awareness, providing vaccines, and allocating additional funds to combat the virus spread (40). Subsequently, the outbreak transitioned from an upsurge phase to a slowdown phase. By 2023 May 11, the WHO declared that mpox no longer constituted a public health emergency, citing a continued decline in reported cases.

$$\begin{aligned}
\frac{dS_1(t)}{dt} &= -\phi_1(t) - \lambda_s^m(t)\langle k_1\rangle S_1(t)\Theta_1'(t) - \lambda_n(t)\langle k_3\rangle S_1(t)\Theta_3'(t),\\
\frac{dS_2(t)}{dt} &= -\phi_2(t) - \lambda_s^o(t)\langle k_2\rangle S_2(t)\Theta_2'(t) - \lambda_n(t)\langle k_3\rangle S_2(t)\Theta_3'(t),\\
\frac{dV_1^1(t)}{dt} &= \phi_1(t) - \psi_1(t) - \epsilon_1\lambda_s^m(t)\langle k_1\rangle V_1^1(t)\Theta_1'(t) - \epsilon_1\lambda_n(t)\langle k_3\rangle V_1^1(t)\Theta_3'(t),\\
\frac{dV_2^1(t)}{dt} &= \phi_2(t) - \psi_2(t) - \epsilon_1\lambda_s^o(t)\langle k_2\rangle V_2^1(t)\Theta_2'(t) - \epsilon_1\lambda_n(t)\langle k_3\rangle V_2^1(t)\Theta_3'(t),\\
\frac{dV_1^2(t)}{dt} &= \psi_1(t) - \epsilon_2\lambda_s^m(t)\langle k_1\rangle V_1^2(t)\Theta_1'(t) - \epsilon_2\lambda_n(t)\langle k_3\rangle V_1^2(t)\Theta_3'(t),\\
\frac{dV_2^2(t)}{dt} &= \psi_2(t) - \epsilon_2\lambda_s^o(t)\langle k_2\rangle V_2^2(t)\Theta_2'(t) - \epsilon_2\lambda_n(t)\langle k_3\rangle V_2^2(t)\Theta_3'(t),\\
\frac{dE_1(t)}{dt} &= (S_1(t) + \epsilon_1 V_1^1(t) + \epsilon_2 V_1^2(t))(\lambda_s^m(t)\langle k_1\rangle\Theta_1'(t) + \lambda_n(t)\langle k_3\rangle\Theta_3'(t)) - \omega E_1(t),\\
\frac{dE_2(t)}{dt} &= (S_2(t) + \epsilon_1 V_2^1(t) + \epsilon_2 V_2^2(t))(\lambda_s^o(t)\langle k_2\rangle\Theta_2'(t) + \lambda_n(t)\langle k_3\rangle\Theta_3'(t)) - \omega E_2(t),\\
\frac{dI_1(t)}{dt} &= \omega E_1(t) - \delta I_1(t),\\
\frac{dI_2(t)}{dt} &= \omega E_2(t) - \delta I_2(t),\\
\frac{dR_1(t)}{dt} &= \delta I_1(t),\\
\frac{dR_2(t)}{dt} &= \delta I_2(t).
\end{aligned} \tag{5}$$

Consequently, we compile weekly confirmed cases and data of vaccination, dividing the model into three phases. The first stage, from 2022 May 28 to 2022 July 30, represents the initial development phase of the mpox epidemic. The second stage, from 2022

August 6 to 2023 May 6, is the slow growth phase, characterized by government interventions such as publicizing the severity of the epidemic through the media, increasing the availability of vaccines, and ramping up vaccination efforts. The third stage, from 2023 May 13 to 2023 September 16, marks the subsequent rebound phase resulting from eased policies. Accordingly, we adapt the time-varying homogeneous model (Eq. 5) to explore human behavior changes during US mpox epidemic. We assume that the MSM and non-MSM populations are vaccinated proportionally:

$$\begin{aligned}\phi_1(t) &= q\phi(t),\\ \phi_2(t) &= (1-q)\phi(t),\\ \psi_1(t) &= q\psi(t),\\ \psi_2(t) &= (1-q)\psi(t).\end{aligned} \tag{6}$$

We denote three time-varying transmission rates as $\beta_s^m(t) = \lambda_s^m(t)\langle k_1\rangle$, $\beta_s^o(t) = \lambda_s^o(t)\langle k_2\rangle$, and $\beta_n(t) = \lambda_n(t)\langle k_3\rangle$. Detailed parameter values for the time-varying transmission rates and the number of vaccinations per week ($\phi(t)$ and $\psi(t)$) are provided in the SI Appendix, Section S3.

Acknowledgment

AI tools have been used to refine the English style of the presentation.

Supplementary Material

Supplementary material is available at *PNAS Nexus* online.

Funding

This work is supported by National Natural Science Foundation of China (grant nos. 12022113 and 12126416), Graduate Innovation Project in Shanxi Province (grant no. 2022Y587) and Fundamental Research Program of Shanxi Province (grant no. 202303021223009). S.B. also acknowledges support from the project no. PGR01177 of the Italian Ministry of Foreign Affairs and International Cooperation.

Author Contributions

W.Z., J.Z., Q.-H.L., S.Z., W.-Q.L., J.-J.M., X.L., S.B., and G.-Q.S. designed the research project. W.Z., J.Z., Q.-H.L., and S.Z. performed the study. W.-Q.L., J.-J.M., X.L., S.B., and G.-Q.S. developed the mathematical formalism. S.B. and G.-Q.S. jointly supervised the research. All authors jointly wrote and reviewed the manuscript.

Data Availability

All study data are included in the article and/or SI Appendix.

References

1 World Health Organization (WHO). Who recommends new name for monkeypox disease; 2022 [accessed 2023 Feb 10]. https://www.who.int/news/item/28-11-2022-who-recommends-new-name-for-monkeypox-disease.
2 Zumla A, *et al.* 2022. Monkeypox outbreaks outside endemic regions: scientific and social priorities. *Lancet Infect Dis*. 22(7): 929–931.
3 Minhaj FS, *et al.* 2022. Monkeypox outbreak—Nine states, May 2022. *Am J Transplant*. 22(8):2104–2110.
4 De Baetselier I, *et al.* 2022. Retrospective detection of asymptomatic monkeypox virus infections among male sexual health clinic attendees in Belgium. *Nat Med*. 28(11):2288–2292.
5 Alakunle EF, Okeke MI. 2022. Monkeypox virus: a neglected zoonotic pathogen spreads globally. *Nat Rev Microbiol*. 20(9):507–508.
6 World Health Organization (WHO). Mpox (monkeypox) outbreak 2022 - global; 2022 [accessed 2023 Feb 10]. https://www.who.int/emergencies/situations/monkeypox-oubreak-2022.
7 World Health Organization (WHO). Mpox (monkeypox); 2022 [accessed 2023 Feb 10]. https://www.who.int/news-room/fact-sheets/detail/monkeypox.
8 World Health Organization (WHO). 2022-23 mpox (monkeypox) outbreak: Global trends; 2022 [accessed 2023 Feb 10]. https://worldhealthorg.shinyapps.io/mpx_global.
9 Takhar SS. 2023. Epidemiologic and clinical characteristics of monkeypox cases – United States, May 17 - July 22, 2022. *Ann Emerg Med*. 81(1):31–34.
10 Patel A, *et al.* 2022. Clinical features and novel presentations of human monkeypox in a central London centre during the 2022 outbreak: descriptive case series. *BMJ*. 378:e072410.
11 Tarín-Vicente EJ, *et al.* 2022. Clinical presentation and virological assessment of confirmed human monkeypox virus cases in Spain: a prospective observational cohort study. *Lancet*. 400(10353): 661–669.
12 Girometti N, *et al.* 2022. Demographic and clinical characteristics of confirmed human monkeypox virus cases in individuals attending a sexual health centre in London, UK: an observational analysis. *Lancet Infect Dis*. 22(9):1321–1328.
13 Bragazzi NL, *et al.* 2022. Epidemiological trends and clinical features of the ongoing monkeypox epidemic: a preliminary pooled data analysis and literature review. *J Med Virol*. 95(1):e27931.
14 Liu X, *et al.* 2022. Monkeypox claims new victims: the outbreak in men who have sex with men. *Infect Dis Poverty*. 11(1):91–93.
15 Spicknall IH, *et al.* 2022. Modeling the impact of sexual networks in the transmission of monkeypox virus among gay, bisexual, and other men who have sex with men – United States, 2022. *Morb Mortal Wkly Rep*. 71(35): 1131–1135.
16 Peter OJ, *et al.* 2022. Transmission dynamics of monkeypox virus: a mathematical modelling approach. *Model Earth Syst Environ*. 8(3): 3423–3434.
17 Peter OJ, *et al.* 2022. Fractional order mathematical model of monkeypox transmission dynamics. *Phys Scr*. 97(8): 084005.
18 Yuan P, *et al.* 2023. Assessing transmission risks and control strategy for monkeypox as an emerging zoonosis in a metropolitan area. *J Med Virol*. 95(1):e28137.
19 Rimoin AW, *et al.* 2010. Major increase in human monkeypox incidence 30 years after smallpox vaccination campaigns cease in the democratic republic of congo. *Proc Natl Acad Sci U S A*. 107(37): 16262–16267.
20 Earl PL, *et al.* 2008. Rapid protection in a monkeypox model by a single injection of a replication-deficient vaccinia virus. *Proc Natl Acad Sci U S A*. 105(31):10889–10894.
21 Bhunu CP, Mushayabasa S, Hyman JM. 2012. Modelling HIV/AIDS and monkeypox co-infection. *Appl Math Comput*. 218:9504–9518.
22 Khan A, Sabbar Y, Din A. 2022. Stochastic modeling of the monkeypox 2022 epidemic with cross-infection hypothesis in a highly disturbed environment. *Math Biosci Eng*. 19(12):13560–13581.
23 Sitaula C, Shahi TB. 2022. Monkeypox virus detection using pre-trained deep learning-based approaches. *J Med Syst*. 46(11):78.
24 Endo A, *et al.* 2022. Heavy-tailed sexual contact networks and monkeypox epidemiology in the global outbreak, 2022. *Science*. 378(6615):90–94.

25 Khaloufi I, Benfatah Y, Laarabi H, Rachik M. 2022. A scenario to fight monkeypox using a mathematical model. *Commun Math Biol Neurosci*. 2022:99.

26 Sood M, *et al.* 2023. Spreading processes with mutations over multilayer networks. *Proc Natl Acad Sci U S A*. 120(24): e2302245120.

27 Brauer F. Compartmental models in epidemiology. 2008. In: Brauer F, Van den Driessche P, Wu J, editors. *Mathematical epidemiology*. Springer. p. 19–79.

28 Newman MEJ. 2002. Spread of epidemic disease on networks. *Phys Rev E*. 66:016128.

29 Kenah E, Robins JM. 2007. Second look at the spread of epidemics on networks. *Phys Rev E*. 76:036113.

30 Bragazzi NL, *et al.* 2023. Adaptive changes in sexual behavior in the high-risk population in response to human monkeypox transmission in Canada can help control the outbreak: insights from a two-group, two-route epidemic model. *J Med Virol*. 95:e28575.

31 Ferguson N. 2007. Capturing human behaviour. *Nature*. 446: 733–733.

32 Bauch C, d'Onofrio A, Manfredi P. Behavioral epidemiology of infectious diseases: an overview. 2013. In: Manfredi P, d'Onofrio A, editors. *Modeling the interplay between human behavior and the spread of infectious diseases*. Springer. p. 1–19.

33 Fu F, Christakis NA, Fowler JH. 2017. Dueling biological and social contagions. *Sci Rep*. 7(1):43634.

34 Fu F, Rosenbloom DI, Wang L, Nowak MA. 2011. Imitation dynamics of vaccination behaviour on social networks. *Proc Royal Soc B*. 278(1702):42–49.

35 Chen X, Fu F. 2019. Imperfect vaccine and hysteresis. *Proc Royal Soc B*. 286(1894):20182406.

36 Zhang H, Wu Z, Tang M, Lai Y. 2014. Effects of behavioral response and vaccination policy on epidemic spreading-an approach based on evolutionary-game dynamics. *Sci Rep*. 4(1):5666.

37 Kabir KMA. 2023. Behavioral vaccination policies and game-environment feedback in epidemic dynamics. *Sci Rep*. 13:14520.

38 Akhmetzhanov AR, Ponce L, Thompson RN. 2022. Emergence potential of monkeypox in the Western Pacific Region, July 2022. *Int J Infect Dis*. 122:829–831.

39 Johnson PLF, *et al.* 2022. Evolutionary consequences of delaying intervention for monkeypox. *Lancet*. 400:1191–1193.

40 The Washington Post. Monkeypox is 'a public health emergency,' U.S. health secretary declares; 2022 [accessed 2023 Feb 10]. https://www.washingtonpost.com/health/2022/08/04/monkeypox-public-health-emergency-united-states-becerra/.

41 U.S. Department of Health and Human Services. Biden-Harris administration bolsters monkeypox response; HHS secretary becerra declares public health emergency; 2022 [accessed 2023 Feb 10]. https://www.hhs.gov/about/news/2022/08/04/biden-harris-administration-bolsters-monkeypox-response-hhs-secretary-becerra-declares-public-health-emergency.html.

42 Brand SPC, *et al.* 2023. The role of vaccination and public awareness in forecasts of mpox incidence in the United Kingdom. *Nat Commun*. 14(1):4100.

43 Kupferschmidt K. 2022. Why monkeypox is mostly hitting men who have sex with men. *Science*. 376(6600):1364–1365.

44 Baggaley RF, White RG, Boily MC. 2010. HIV transmission risk through anal intercourse: systematic review, meta-analysis and implications for HIV prevention. *Int J Epidemiol*. 39(4): 1048–1063.

45 Patel P, *et al.* 2014. Estimating per-act HIV transmission risk: a systematic review. *Aids*. 28(10):1509–1519.

46 Borges V, *et al.* 2023. Viral genetic clustering and transmission dynamics of the 2022 mpox outbreak in Portugal. *Nat Med*. 29(10): 2509–2517.

47 Liljeros F, Edling CR, Amaral LAN, Stanley HE, Åberg Y. 2001. The web of human sexual contacts. *Nature*. 411:907–908.

48 Schneeberger A, *et al.* 2004. Scale-free networks and sexually transmitted diseases: a description of observed patterns of sexual contacts in Britain and Zimbabwe. *Sex Transm Dis*. 31: 380–387.

49 Whittles LK, White PJ, Didelot X. 2019. A dynamic power-law sexual network model of gonorrhoea outbreaks. *PLoS Comput Biol*. 15: e1006748.

50 Kollepara PK, Chisholm RH, Miller JC. 2023. Heterogeneity in network structure switches the dominant transmission mode of infectious diseases. *PNAS Nexus*. 2(8):pgad227.

51 Mossong J, *et al.* 2008. Social contacts and mixing patterns relevant to the spread of infectious diseases. *PLoS Med*. 5(3):e74.

52 Delamater PL, Street EJ, Leslie TF, Yang YT, Jacobsen KH. 2019. Complexity of the basic reproduction number (R0). *Emerging Infect Dis*. 25(1):1–4.

53 Centers for Disease Control and Prevention. Technical report 4: multi-national mpox outbreak, United States, 2022; 2022 [accessed 2023 Feb 10]. https://www.cdc.gov/poxvirus/mpox/cases-data/technical-report/report-4.html.

54 World Health Organization (WHO). Third meeting of the international health regulations (2005) (IHR) emergency committee regarding the multi-country outbreak of monkeypox; 2022 [accessed 2023 February 10]. https://www.who.int/news/item/01-11-2022-third-meeting-of-the-international-health-regulations-(2005)-(ihr)-emergency-committee-regarding-the-multi-country-outbreak-of-monkeypox.

55 Chan HF, Skali A, Savage DA, Stadelmann D, Torgler B. 2020. Risk attitudes and human mobility during the COVID-19 pandemic. *Sci Rep*. 10(1):19931.